ELECTRONIC SUPPLEMENTARY INFORMATION

Confining perovskite quantum dots in the pores of a covalent-organic framework: quantum confinement- and passivation-enhanced light-harvesting and photocatalysis

Genping Meng, Liping Zhen, Shihao Sun, Jun Hai,* Zefan Zhang, Dina Sun, Qiang Liu,* and Baodui Wang*

State Key Laboratory of Applied Organic Chemistry and Key Laboratory of Nonferrous Metal Chemistry and Resources Utilization of Gansu Province, Lanzhou University, Gansu, Lanzhou, 730000. China.

Email: haij@lzu.edu.cn; liuqiang@lzu.edu.cn; wangbd@lzu.edu.cn

Experimental Section

Materials. All reactions were performed in air atmosphere unless otherwise stated. The commercially available reagents and solvents were either employed as purchased or dried according to the procedures described in literature. Lead chloride ($PbCl_2$, 100.0%), Lead bromide ($PbBr_2$, 99.0%), Lead iodide (PbI_2, 99.99%) were purchased from ITC, Octadecene (ODE, 90%), oleic acid (OA, 90%) were obtained from Sigma. 1,3,5-Tris(4-aminophenyl)benzene (TPB) was obtained from Jilin Chinese Academy of Sciences-Yanshen Technology Co., Ltd.

Measurements. Transmission electron microscopy (TEM) and high-resolution TEM were performed on a FEI Tecna i-G2-F30 electron microscope operating at an accelerating voltage of 200 kV. Samples for TEM analysis were prepared by dropping a dilute solution of composites in acetonitrile onto ultrathin carbon-coated copper grids. Morphology of samples were performed by Field emission Scanning Electron Microscope (SEM, FEI, Sirion 200) with an accelerating voltage of 15 kV. Powdered X-ray diffraction (PXRD) patterns were recorded on AXS D8-Advanced diffractometer with Cu Ka radiation. The nitrogen adsorption-desorption isotherms were acquired through a high precision Autosorb apparatus at 77.35 K, and Non-Local Density Functional Theory (NLDFT) method was applied to the adsorption branch to calculate the pore size distribution of COFs. X-ray photoelectron spectroscopy (XPS, a PHI5702 multifunctional spectrometer) measurements were investigated on a PHI-5702 multifunctional spectrometer using Al Kα radiation. Fourier transform infrared (FTIR) spectra were recorded with a Nicolet FT-170SX spectrometer at room temperature. Ultraviolet and visible absorption (UV-vis) spectra were recorded on Shimadzu UV-1750 at room temperature. Photocatalysis was performed using Xenon lamp (HSXF/UV 300), equipped with 400-800 nm filter. Photoluminescence (PL) spectra were acquired on an Edinburgh Instruments FLS920 fluorescence spectrometer. ^{1}H-NMR spectra were gathered on a JEOL ESC 400 M instrument with tetramethylsilane as the internal standard. The standard silica particles samples dispersed in water were used as the standard to eliminate the effect of the scattering from the samples. Time-resolved PL decay curves were fitted to a biexponential (see **eqs S1** and **S2**) decay curves of

$$A(t) = A_1 \exp\left(-\frac{t}{\tau_1}\right) + A_2 \exp\left(-\frac{t}{\tau_2}\right) \qquad \textbf{eq S1}$$

The average lifetimes were calculated using

$$\tau_{avg} = (A_1{\tau_1}^2 + A_2{\tau_2}^2)/(A_1\tau_1 + A_2\tau_2) \qquad \textbf{eq S2}$$

The detailed synthetic methods including the monomers and COFs are given as follows:

Synthesis of 2,5-dibromobenzene-1,4-dicarbaldehyde.

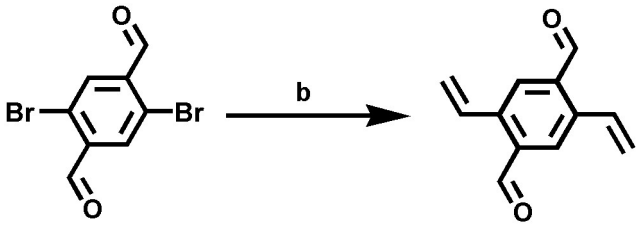

Reagent b: $Pd(PPh_3)_4$, potassium vinyltrifluoroborate

The 2,5-dibromobenzene-1,4-dicarbaldehyde was prepared according to the previous literature with some modification.[1] To a mixture of 1,4-dibromo-2,5-dimethylbenzene (303 mmol, 8 g), acetic acid (40 mL), acetic anhydride (80 mL) at 0 °C, sulfuric acid (28 mL) was added dropwise. CrO_3 (120 mmol,12 g) was then added to the mixture in small portions. The resultant mixture was stirred at 0 °C overnight. The greenish slurry was poured into ice water, filtrated, and washed with water and methanol. The obtained diacetate was then hydrolyzed by refluxing with a mixture of water (40 mL), ethanol (40 mL) and sulfuric acid (4 mL) overnight. The title product was obtained by filtration, which was used directly for the next step without further purification. Yield: 3.18 g (36.0%).

Synthesis of 2,5-divinylterephthalaldehyde

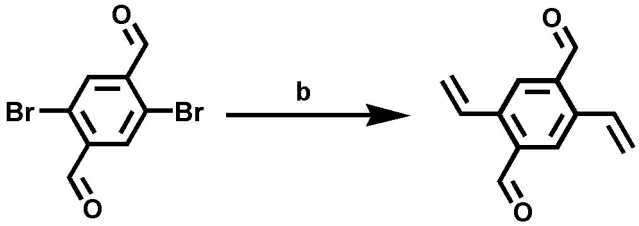

Reagent b: $Pd(PPh_3)_4$, potassium vinyltrifluoroborate

The 2,5-divinylterephthalaldehyde was synthesized according to the previous literature.[1] 2,5-dibromobenzene-1,4-dicarbaldehyde (13.7 mmol, 4.0 g), potassium vinyltrifluoroborate (33.1 mmol, 4.57 g), K_2CO_3 (82.2 mmol, 11.3 g), and $Pd(PPh_3)_4$ (0.411 mmol, 0.456 g) were dissolved in a mixture of toluene (50 mL), THF (50 mL) and H_2O (10 mL), the resulting mixture was refluxed at 90 °C under N_2 atmosphere for 24 h. The residue was extracted with ethyl acetate, washed with brine, dried over Na_2SO_4, and evaporated under reduced pressure, giving the crude compound which was purified by flash chromatography with hexane/ethyl acetate (10:1) as eluent to afford the title compound as yellow solid. Yield: 1.83 g (71.7%). ^1H NMR (400 MHz, $CDCl_3$, 298K, TMS): δ 10.37 (s, 2H), 8.01 (s, 2H), 7.49 (dd, J = 17.4, 11.0 Hz, 2H), 5.81 (d, 2H, J=17.4 Hz), 5.60 (d, 2H, J=11.0 Hz) ppm (Figure S18).

Synthesis of Cs-Oleate. Cs-Oleate (CsOA) was synthesized according to the previous literature.[2] Oleic acid (2.5 mL) and octadecene (10 mL, ODE) were syringed into a 100 mL 3-neck flask containing 0.814 g of Cs_2CO_3 (2.50 mmol). The resulting mixture was dried at 120 °C for 1 h and then reacted at 150 °C under N_2 atmosphere for 2h. Since CsOA will precipitate out of ODE at room temperature, it has to be preheated to dissolve before usage.

Energy transfer efficiency (Φ_{ET}) calculation[3]

The energy-transfer efficiency (Φ_{ET}) was calculated using equation **S3**:

$\Phi_{ET} = 1 - I_{DA}$, (λ_{ex} = donor)/I_D, (λ_{ex} = donor) **(eq. S3)**

For ESY-$CsPbBr_3$@COF-SH system, where I_{DA} and I_D are the fluorescence intensities of

ESY- $CsPbBr_3$@COF-SH (donor and acceptor) and $CsPbBr_3$@COF-SH composite (donor) at 514 nm when excited at 365 nm, respectively. The energy-transfer efficiency ($\mathbf{\Phi_{ET}}$) was calculated as 94.4% in MeCN, measured under the condition of [$CsPbBr_3$@COF-SH] = 3.13×10^{-5} M, [ESY] = 1.54×10^{-3} M, and λ_{ex} = 365 nm.

For RB-$CsPbBr_2I$@COF-SH system, where $\mathbf{I_{DA}}$ and $\mathbf{I_D}$ are the fluorescence intensities of RB-$CsPbBr_2I$@COF-SH (donor and acceptor) and $CsPbBr_2I$@COF-SH composite (donor) at 536 nm when excited at 365 nm, respectively. The energy-transfer efficiency ($\mathbf{\Phi_{ET}}$) was calculated as 93.6% in MeCN, measured under the condition of [$CsPbBr_2I$@COF-SH] = 3.13×10^{-5} M, [RB] = 3.14×10^{-3} M, and λ_{ex} = 365 nm.

Photoluminescence Quantum Yield ($\mathbf{\Phi_{PLQY}}$) calculation

The PLQY was measured at room temperature with fluorescein in 0.1 M NaOH (Φ_{PLQY} = 0.89) as standard. The PLQY can be calculated using the following equation **S4**:[4]

$$\Phi = \Phi_R \frac{\int F(\lambda_{em})\, A_R(\lambda_{ex})\, n^2}{\int F_R(\lambda_{em})\, A(\lambda_{ex})\, {n_R}^2} \qquad \textbf{(eq. S4)}$$

where Φ is the PLQY, $\int F(\lambda_{em})$ is the integrated intensity of emission, $A(\lambda_{ex})$ is the percentage of light absorbed at excitation wavelength, n is the refractive index, and subscript R denoted the reference data.[5]

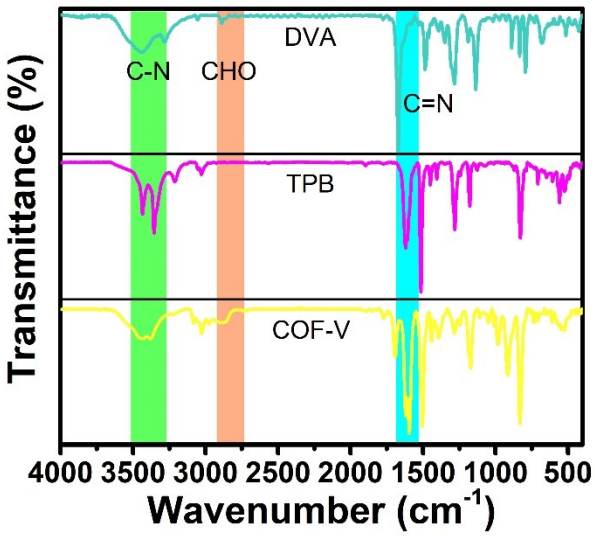

Figure S1. FT-IR spectra of COF-V (blue), DVA (cyan) and TPB (orange).

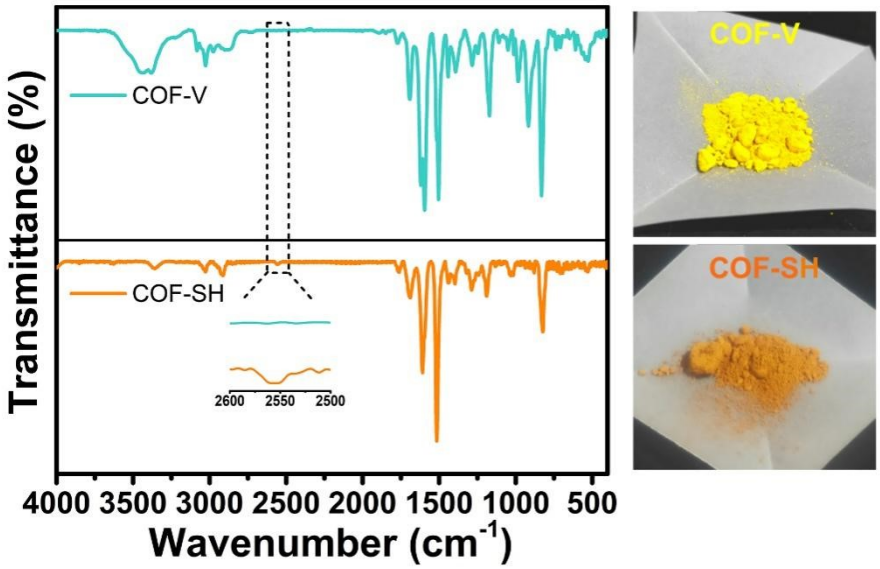

Figure S2. FT-IR spectra of COF-V (cyan) and COF-SH (orange).

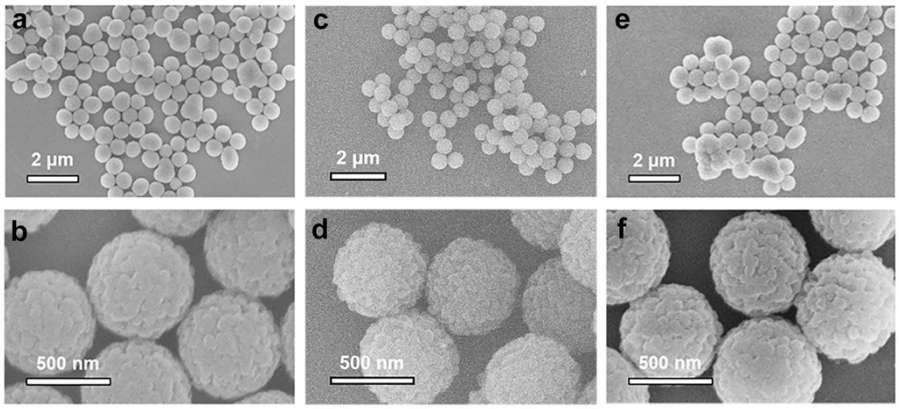

Figure S3. (a, b) SEM images of COF-V. (c, d) SEM images of COF-SH. (e, f) SEM images of $CsPbBr_3$@COF-SH

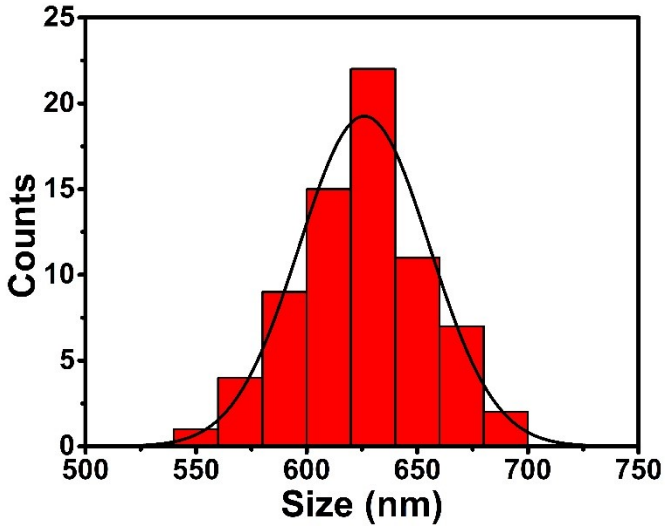

Figure S4. Size distribution of COF-V.

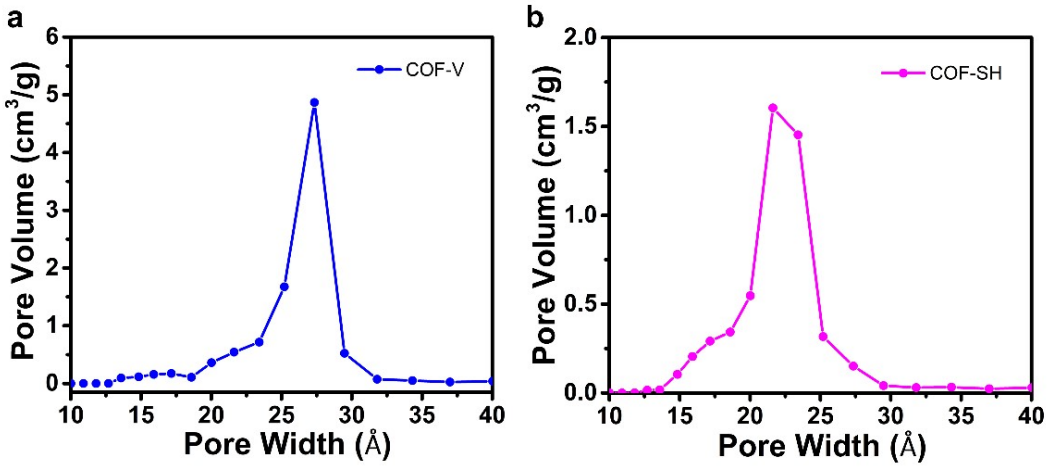

Figure S5. (a, b) Pore size distribution of spherical COF-V and COF-SH calculation based upon NLDFT.

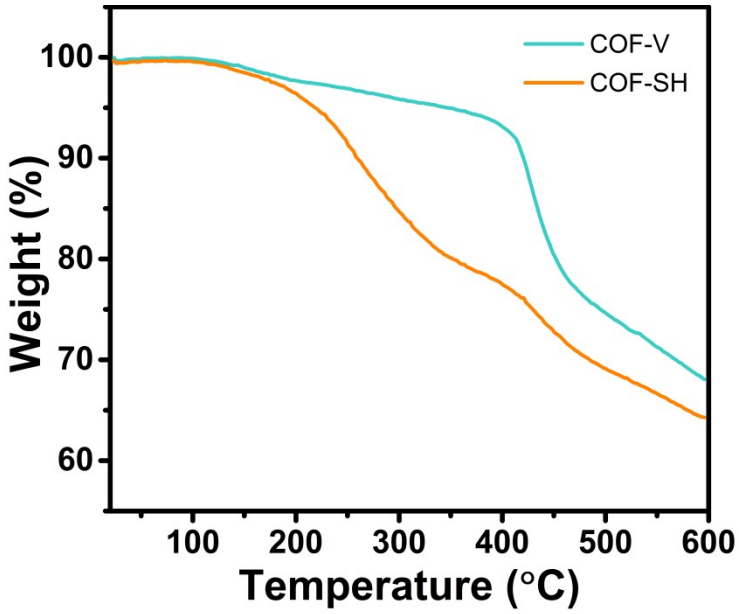

Figure S6. Thermo gravimetric analysis (TGA) of COF-V (cyan) and COF- SH (orange)

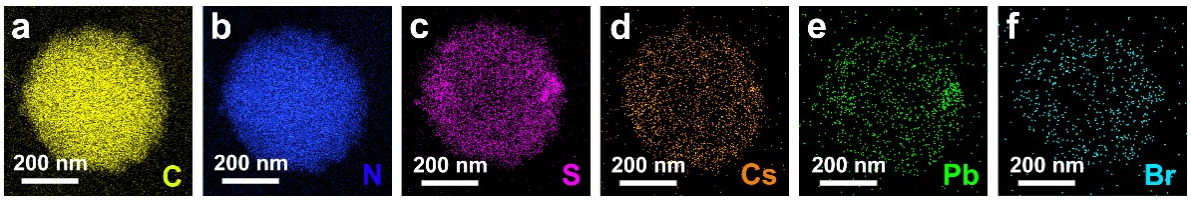

Figure S7. Elemental mapping by EDX for $CsPbBr_3$@COF-SH composite in **Figure 2d**

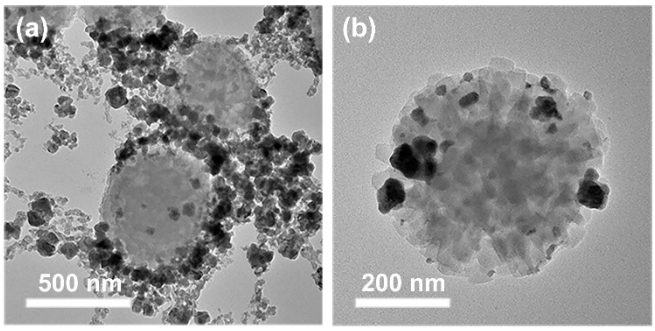

Figure S8. (a, b) TEM images of $CsPbBr_3$-COF-V

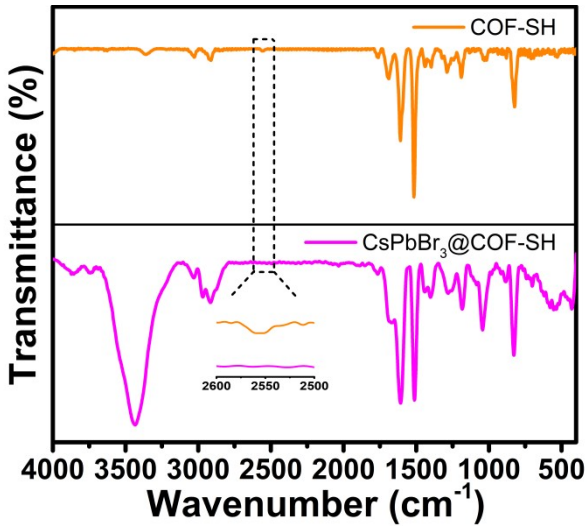

Figure S9. FT-IR spectra of COF-SH (orange) and $CsPbBr_3$@COF-SH composite (purple).

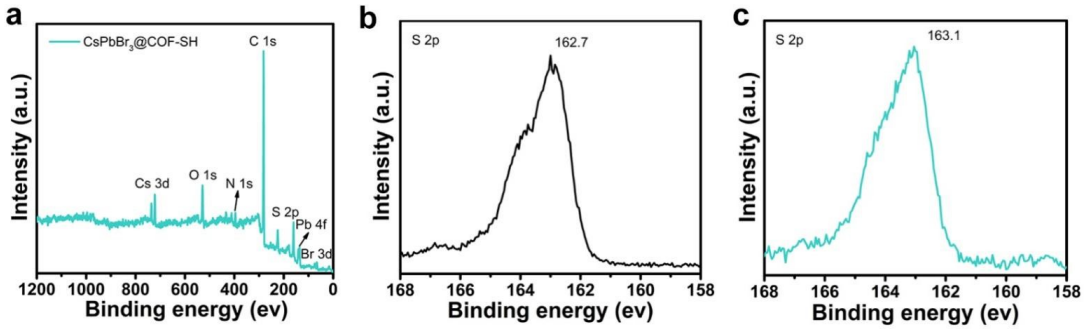

Figure S10. (a) XPS spectra of the $CsPbBr_3$@COF-SH composite. S 2p XPS spectra of the (b) COF-SH and (c) $CsPbBr_3$@COF-SH composite.

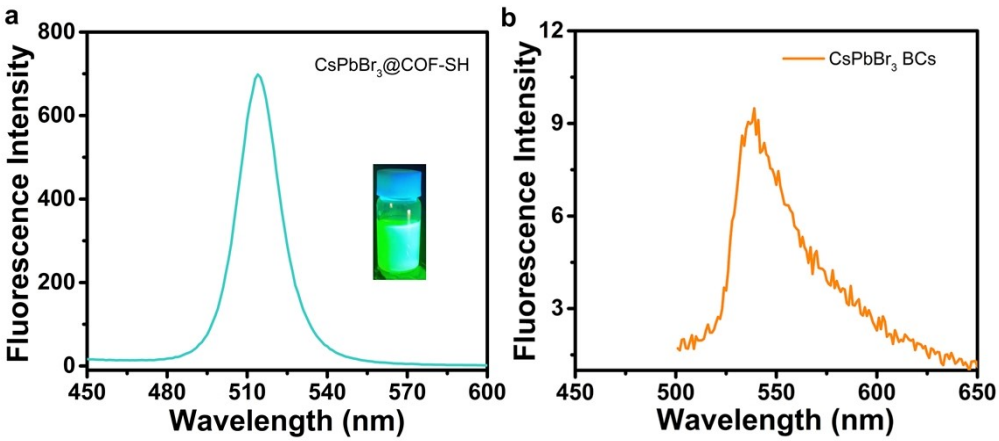

Figure S11. (a) Emission spectrum of $CsPbBr_3$@COF-SH composite in MeCN. (b) Emission spectrum of $CsPbBr_3$ BCs in MeCN.

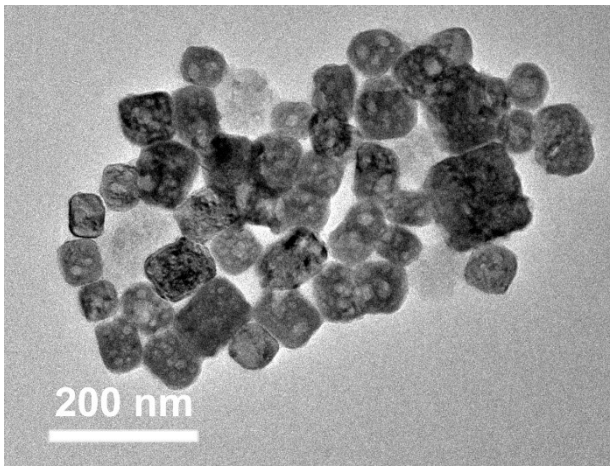

Figure S12. TEM image of the $CsPbBr_3$ BCs.

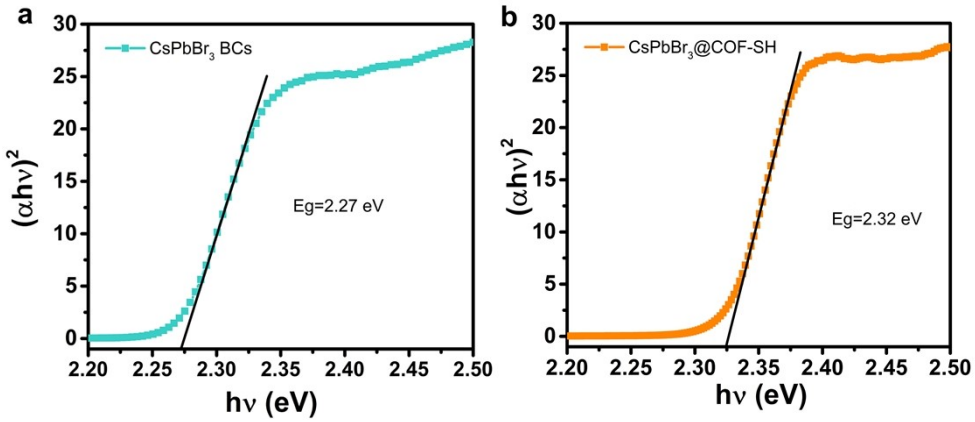

Figure S13. Tauc-plot curves of the (a) $CsPbBr_3$ BCs and (b) $CsPbBr_3$@COF-SH composite.

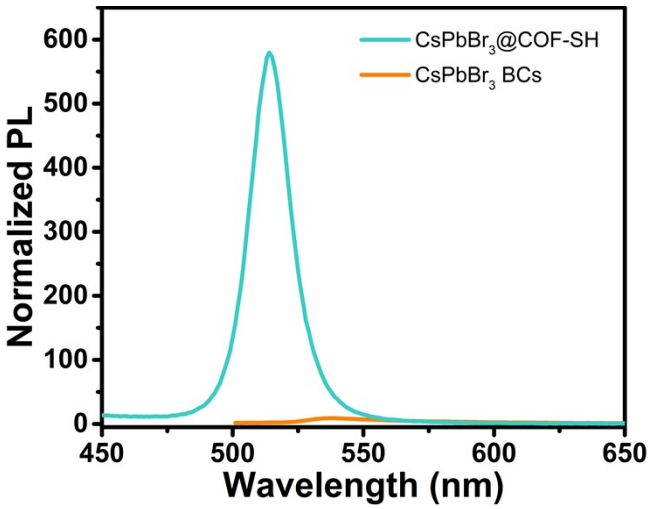

Figure S14. Emission spectra of $CsPbBr_3$@COF-SH composite and $CsPbBr_3$ BCs.

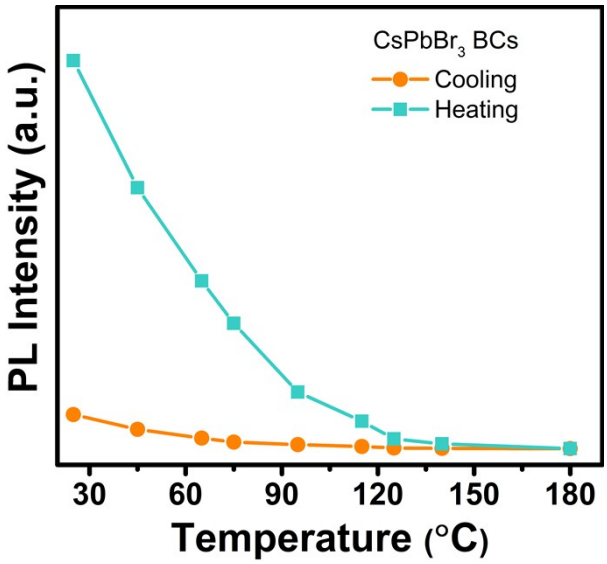

Figure S15. Temperature-dependent PL intensity for $CsPbBr_3$ BCs.

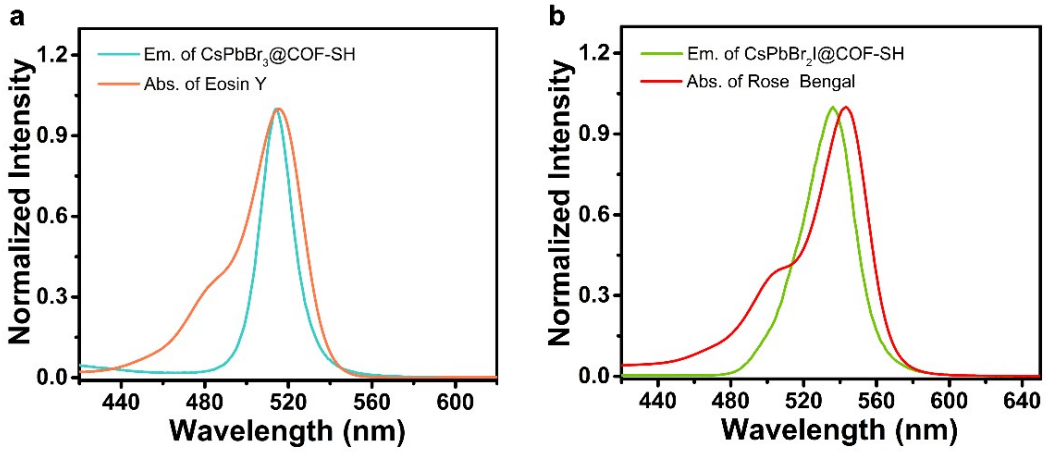

Figure S16. (a) Normalized absorption spectrum of ESY and emission spectrum of $CsPbBr_3$@COF-SH composite. (b) Normalized absorption spectrum of RB and emission spectrum of $CsPbBr_2I$@COF-SH composite.

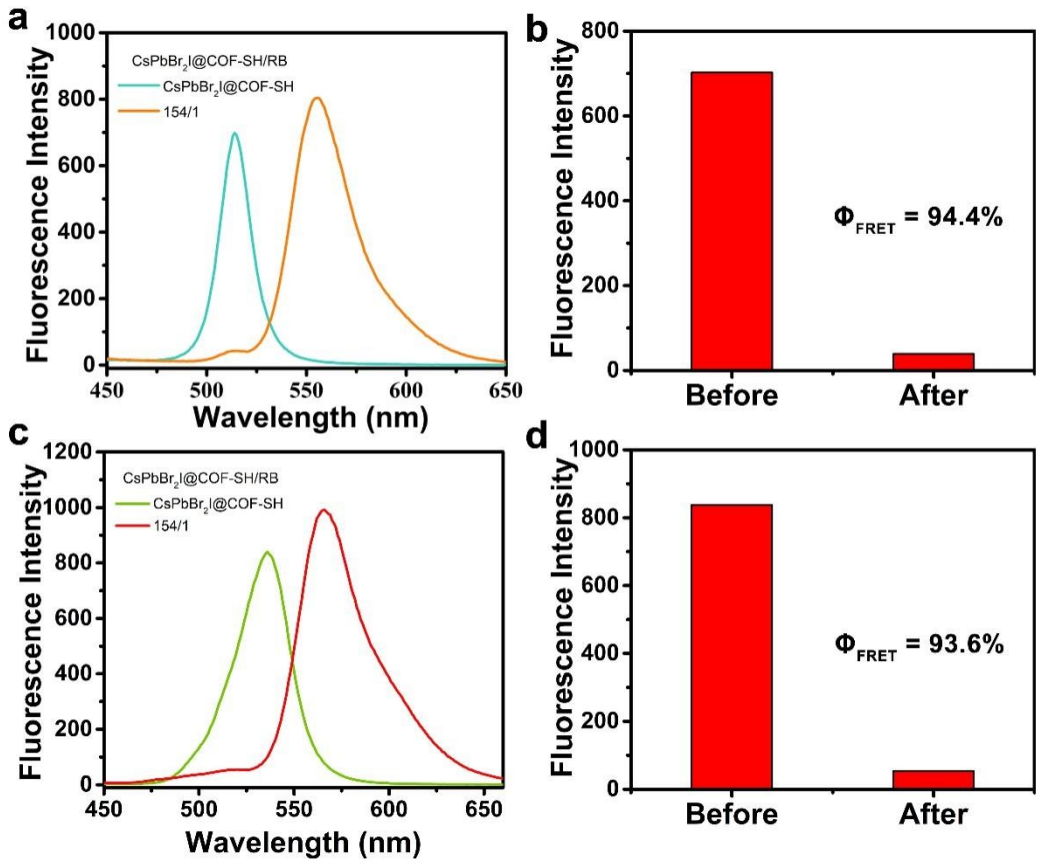

Figure S17. (a) Fluorescence spectra of $CsPbBr_3$@COF-SH composite and ESY-$CsPbBr_3$@COF-SH system. (b) The histogram of $CsPbBr_3$@COF-SH and ESY-$CsPbBr_3$@COF-SH systems emission intensities. (c) Fluorescence spectra of $CsPbBr_2I$@COF-SH composite and RB-$CsPbBr_2I$@COF-SH system. (d) The histogram of $CsPbBr_2I$@COF-SH composite and RB-$CsPbBr_2I$@COF-SH system emission intensities.

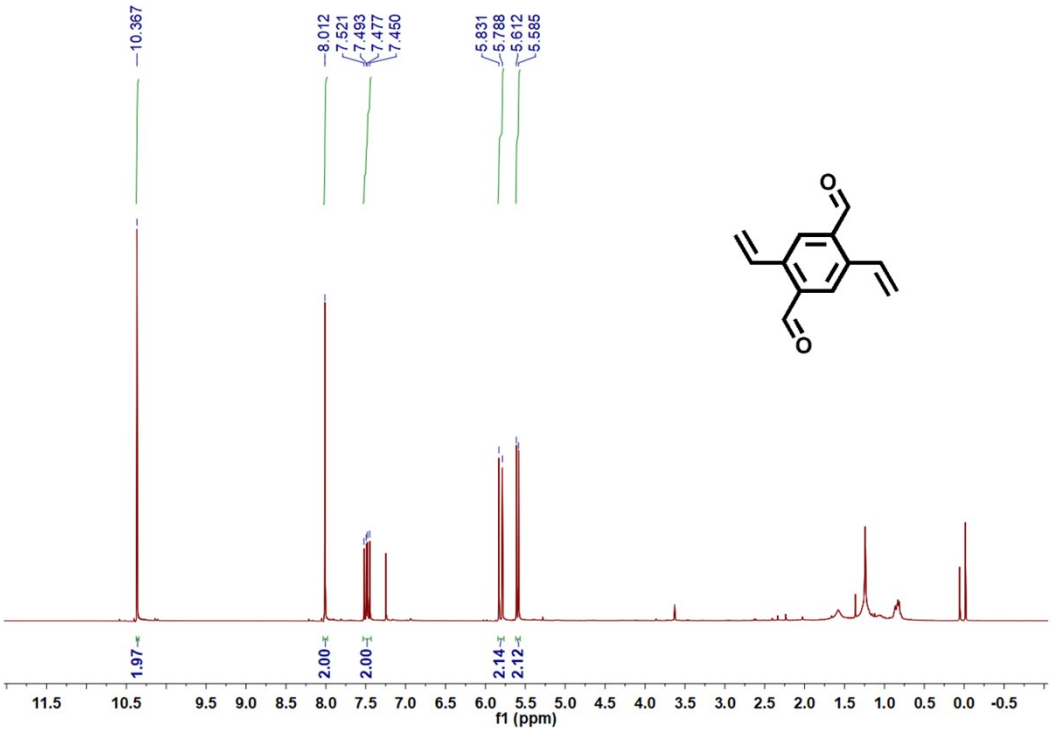

Figure S18. ^{1}H NMR spectrum (400 MHz, $CDCl_3$, 298K) of 2,5-divinylterephthalaldehyde.

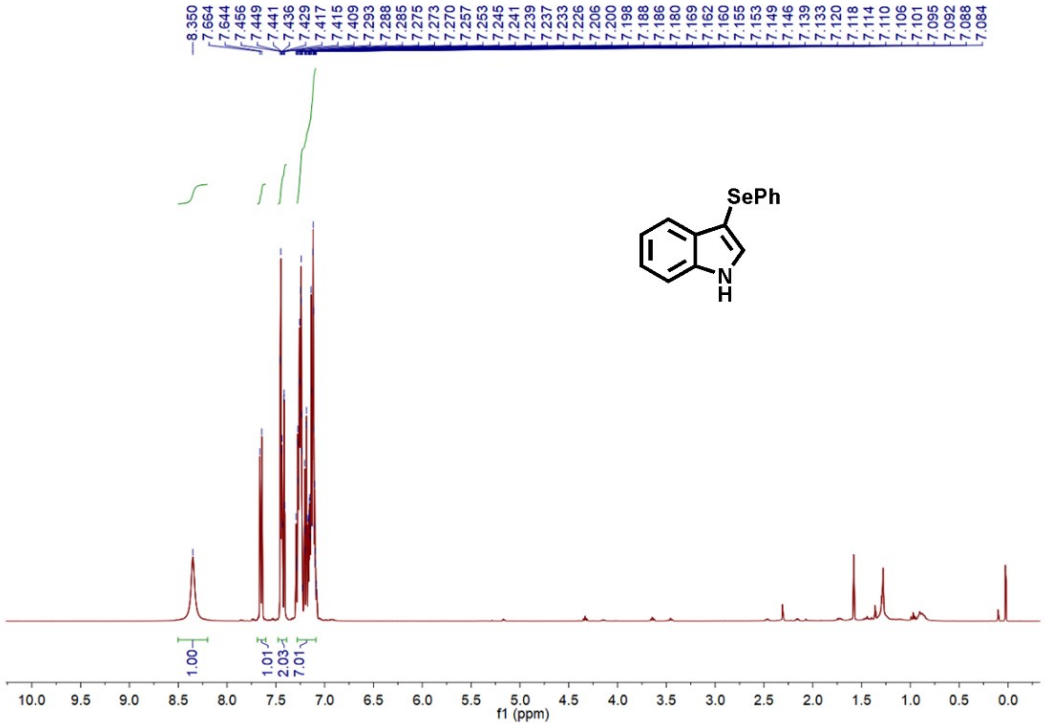

Figure S19. ^{1}H NMR spectrum (400 MHz, $CDCl_3$, 298K) of **3**.

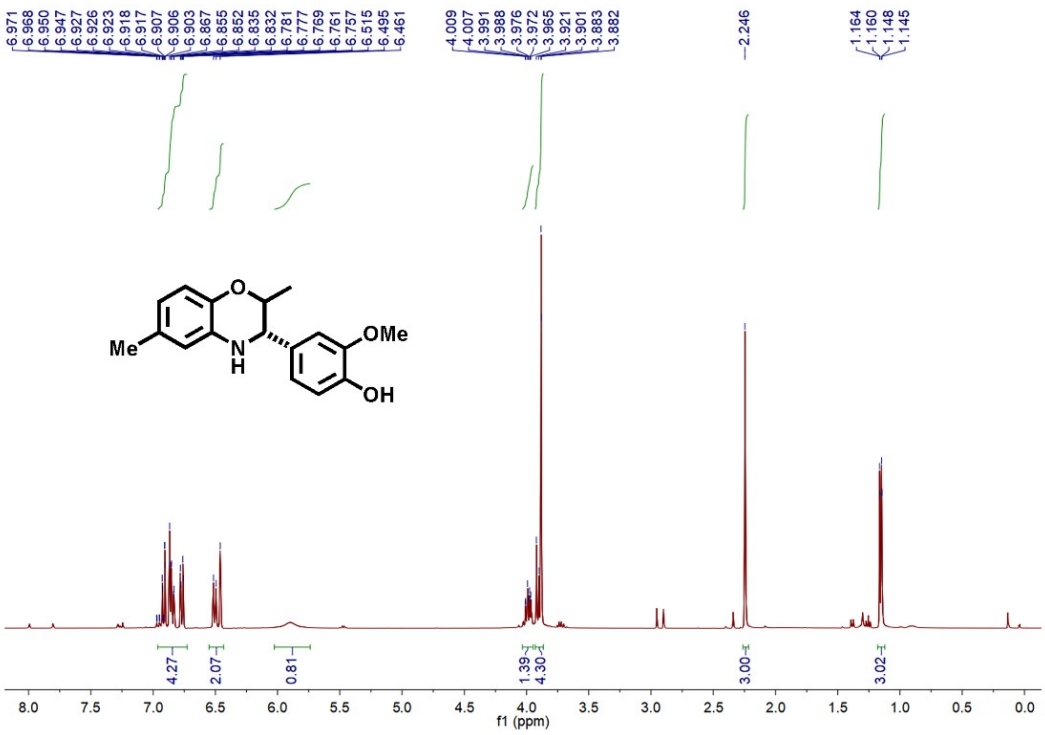

Figure S20. ^{1}H NMR spectrum (400 MHz, $CDCl_3$, 298K) of **6**.

Table S1. Specific surface areas of COF-V and COF-SH scaffold calculated with BET method.

Sample	Specific Surface Area (m^2g^{-1})	Mean pore size (nm)
COF-V	901.5	2.73
COF-SH	551.7	2.25
$CsPbBr_3$@COF-SH	78.4	-

Table S2. TRPL results for $CsPbBr_3$@COF-SH composite and $CsPbBr_3$ BCs.

Sample	τ_1(ns)	Proportion (%)	τ_2(ns)	Proportion (%)	$\tau_{av.}$(ns)
$CsPbBr_3$@COF-SH	7.34	71	56.70	29	21.65
$CsPbBr_3$ BCs	3.27	77	18.25	23	6.72

Table S3. Fluorescence quantum yields of $CsPbBr_3$@COF-SH and $CsPbBr_2I$@COF-SH composites (in MeCN).

Sample	Concentration (M)	Photoluminescence quantum yields (PLQY)
$CsPbBr_3$@COF-SH	3.13×10^{-5}	30.2%
$CsPbBr_2I$@COF-SH	3.13×10^{-5}	27.6%

Table S4. Fluorescence lifetimes of $CsPbBr_3$@COF-SH, ESY-$CsPbBr_3$@COF-SH, $CsPbBr_2I$@COF-SH, and RB-$CsPbBr_2I$@COF-SH in MeCN.

Sample	τ_1(ns)	Proportion (%)	τ_2(ns)	Proportion (%)	$\tau_{av.}$(ns)
$CsPbBr_3$@COF-SH	7.34	71	56.70	29	21.65
ESY-$CsPbBr_3$@COF-SH	1.38	85	8.63	15	2.47
$CsPbBr_2I$@COF-SH	7.73	72	71.05	28	25.46
RB-$CsPbBr_2I$@COF-SH	1.96	86	5.42	14	2.44

Table S5. The energy transfer efficiency in MeCN.

Sample	Donor/acceptor ratio (v/v)	Energy transfer efficiency (Φ_{ET})
ESY-$CsPbBr_3$@COF-SH	154:1	94.4%
RB-$CsPbBr_2I$@COF-SH	154:1	93.6%

[$CsPbBr_3$@COF-SH] = 3.13×10^{-5} M, [ESY] = 1.54×10^{-3} M, [$CsPbBr_2I$@COF-SH] = 3.13×10^{-5} M, [RB] = 3.14×10^{-3} M

Supporting References

1. Q. Sun, B. Aguila, J. Perman, L. D. Earl, C. W. Abney, Y. Cheng, H. Wei, N. Nguyen, L. Wojtas and S. Ma, *J Am Chem Soc*, 2017, **139**, 2786-2793.
2. S. Sun, D. Yuan, Y. Xu, A. Wang and Z. Deng, *ACS Nano*, 2016, **10**, 3648-3657.
3. D. Zhang, W. Yu, S. Li, Y. Xia, X. Li, Y. Li and T. Yi, *J Am Chem Soc*, 2021, **143**, 1313-1317.
4. K. Rurack and M. Spieles, *Anal Chem*, 2011, **83**, 1232-1242.
5. C. Wurth, M. Grabolle, J. Pauli, M. Spieles and U. Resch-Genger, *Nat Protoc*, 2013, **8**, 1535-1550.